Fluorescence Energy Transfer Studies of Human Deoxycytidine Kinase: Role of Cysteine 185 in the Conformational Changes that Occur upon Substrate Binding†

Rajam S. Mani,‡ Elena V. Usova,§ Carol E. Cass,‡ and Staffan Eriksson*,§

Department of Experimental Oncology, Cross Cancer Institute, and Department of Oncology, University of Alberta, Edmonton, Alberta T6G 1Z2, Canada, and Department of Molecular Biosciences, Swedish University of Agricultural Sciences, The Biomedical Centre, SE 753 24 Uppsala, Sweden

Received December 29, 2005; Revised Manuscript Received January 24, 2006

ABSTRACT: Human deoxycytidine kinase (dCK) phosphorylates both pyrimidine and purine deoxynucleosides, including numerous nucleoside analogue prodrugs. Energy transfer studies of transfer between Trp residues of dCK and the fluorescent probe *N*-(1-pyrene)maleimide (PM), which specifically labels Cys residues in proteins, were performed. Two of the six Cys residues in dCK were labeled, yielding a protein that was functionally active. We determined the average distances between PM-labeled Cys residues and Trp residues in dCK in the absence and presence of various pyrimidine and purine nucleoside analogues with the Trp residues as energy donors and PM-labeled Cys residues as acceptors. The transfer efficiency was determined from donor intensity quenching and the Förster distance R_0 at which the efficiency of energy transfer is 50%, which was 19.90 Å for dCK-PM. The average distance *R* between the Trp residues and the labeled Cys residues in dCK-PM was 18.50 Å, and once substrates bound, this distance was reduced, demonstrating conformational changes. Several of the Cys residues of dCK were mutated to Ala, and the properties of the purified mutant proteins were studied. PM labeled a single Cys residue in Cys-185-Ala dCK, suggesting that one of the two Cys residues labeled in wild-type dCK was Cys 185. The distance between the single PM-labeled Cys residue and the Trp residues in Cys-185-Ala dCK was 20.75 Å. Binding of nucleosides had no effect on the pyrene fluorescence of Cys-185-Ala dCK, indicating that the conformational changes observed upon substrate binding to wild-type dCK-PM involved the "lid region" of which Cys 185 is a part. The substrate specificity of Cys-185-Ala dCK was altered in that dAdo and UTP were better substrates for the mutant than for the wild-type enzyme.

Deoxycytidine kinase (dCK,[1] EC 2.7.1.74), a key enzyme in the salvage pathway for deoxynucleosides, catalyzes phosphorylation of a deoxynucleoside to the corresponding monophosphates using nucleoside triphosphates as phosphate donors. dCK also phosphorylates many important anticancer and antiviral drugs (*1*, *2*). The human enzyme is composed of two identical polypeptides of 260 amino acids (*3*, *4*), and its three-dimensional crystal structure was recently reported in complexes with its physiological substrate deoxycytidine (dCyd) and with the prodrugs cytarabine (AraC) or gemcitabine (dFdC) (*5*).

Previous studies have shown that the kinetic behavior of dCK is complex. It phosphorylates both pyrimidine and purine nucleoside analogues but with different apparent substrate affinities. Its reaction kinetics exhibit negative cooperativity with the phosphate acceptors and donors yielding Hill coefficients below unity (*6*, *7*). Kinetic studies at low nucleoside concentrations showed that the reaction was random bi-bi with ATP and ordered with UTP with the donor binding before the acceptor (*8*). Human dCK exhibited a "preference" for UTP in that the K_m values for the nucleoside substrates were usually lower when UTP was used as the phosphate donor instead of ATP (*9*). The mechanism for the influence of phosphate donors on the nucleoside specificity of dCK is not understood but is most likely important for the in vivo function of the enzyme.

Earlier fluorescence quenching studies revealed that substrate binding induced conformational changes (*10*, *11*), suggesting that dCK exists in different conformational states with different affinities for its substrates. Although the three-dimensional crystal structure of dCK defined the determinants for substrate specificity with pyrimidine nucleosides, it is not in accordance with the available kinetic data (*8*) since the structural model places the nucleoside-binding site in the interior and the phosphate donor site on the exterior of the protein and predicts that the phosphate donor binds after the nucleoside substrate. Furthermore, the structure of

† This research was supported by grants from the National Cancer Institute of Canada to C.E.C. and the Swedish Research Council to S.E. and by the Alberta Cancer Board and the Faculty of Medicine and Dentistry of the University of Alberta. C.E.C. is Canada Research Chair in Oncology.

* To whom correspondence should be addressed: Department of Molecular Biosciences, Swedish University of Agricultural Sciences, The Biomedical Centre, P.O. Box 575, SE 753 24 Uppsala, Sweden. Telephone: 46-18-4714178. Fax: 46-18-550762. E-mail: Staffan.Eriksson@vmk.slu.se.

‡ University of Alberta.

§ Swedish University of Agricultural Sciences.

[1] Abbreviations: PM, *N*-(1-pyrene)maleimide; dCK, deoxycytidine kinase; Tris, tris(hydroxymethyl)aminomethane; DTNB, 5,5′-dithiobis-(2-nitrobenzoate); BSA, bovine serum albumin; DTT, dithiothreitol; dFdC, gemcitabine (2′,2′-difluorodeoxycytidine); Fara-A, fludarabine (9-β-D-arabinofuranosyl-2-fluoroadenine).

10.1021/bi052652b CCC: $33.50
Published on Web 02/24/2006

Table 1: Oligonucleotide Primers Used for Site-Directed Mutagenesis[a]

mutation	5′−3′ sense primer	5′−3′ antisense primer
Cys-45-Ala	AAACAATTGGCTGAAGATTGG	CCAATCTTCAGCCAATTGTTT
Cys-101-Ala	ACATATGCCGCTCTCAGTCGA	TCGACTGAGAGCCCGATATGT
Cys-146-Ala	GAATCTGAAGCCCATGAATGAG	CTCATTCATGGCTTCAGATTC
Cys-185-Ala	CCAGAGACAGCCTTACATAGA	TCTATGTAAGGCTGTCTCTGG

[a] The underlined nucleotides correspond to a change from the cysteine codon to an alanine codon.

dCK in complex with purine nucleoside substrates has not been determined, although models have recently been described (*12*).

To resolve the discrepancy between the kinetic results and the structural model, we examined conformational changes in purified human dCK in solution before and after substrate binding by employing fluorescence energy transfer experiments. Energy transfer studies of transfer between Trp residues in dCK and the fluorescent probe *N*-(1-pyrene)-maleimide (PM), which specifically labels Cys residues, were performed using the Trp residues as energy donors and the PM-labeled Cys residues as acceptors. We measured the average distances between the donor and acceptor residues in the absence and presence of various pyrimidine and purine nucleoside analogues and found that these distances were reduced upon substrate binding. Nucleoside analogues were capable of binding to dCK-PM in the presence of phosphate donors, providing evidence of ternary complexes involving dCK-PM, phosphate donors, and nucleoside analogues. Cys 185 is located in the proximity of the nucleotide binding lid region of dCK, and this residue was replaced with Ala (Cys-185-Ala); mutant dCK with Cys residues at positions 101 or 45 converted to Ala were also prepared. The kinetic properties of the various Cys mutants were investigated. PM treatment of Cys-185-Ala, labeled only one Cys residue. Kinetic studies showed that the addition of PM did not have any influence on the enzymatic activity of Cys-185-Ala, although there were changes in substrate specificity.

MATERIALS AND METHODS

Crystal and Nucleoside Structures. The coordinates for dCKc (PDN entry 1p60, resolution of 1.96 Å, *R* value of 0.165, dC substrate) were obtained from the Protein Data Bank.

Site-Directed Mutagenesis. Site-directed mutagenesis was performed according to the method of Ho et al. (*13*). The pET-9d/dCK construct was used as the template DNA for mutagenic PCR. Mutations were produced in two steps with four primers in which the N-terminal NcoI-N and C-terminal BamHI-C primers were identical to those used to generate the pET-9d/dCK insert. Two separate amplification reactions with a NcoI-N primer and a mutant antisense primer and the other mutant sense primer and a BamHI-C primer were performed for each mutant construct. The 21-mer mutagenic primers were used as oligonucleotides for constructing Cys-185-Ala, Cys-146-Ala, Cys-101-Ala, and Cys-45-Ala mutants (Table 1). The reaction products were electrophoresed on a 1% agarose TAE gel; the DNA bands were excised, pooled, and purified using the gel extraction kit (Qiagene GmbH, Hilden, Germany), and the resulting purified plasmid DNA was used as the template for a second PCR amplification with NcoI-N and BamHI-C primers. The resulting 780 bp band was gel-purified and digested with NcoI and BamHI prior to being ligated into the NcoI and BamHI sites of the pET-9d vector. Point mutations were confirmed by cycle sequencing using the ABI Prism BigDye Terminator Cycle Sequencing Ready Reaction Kits and an ABI prism instrument (ABI PRISM 310 Genetic Analyzer, PE Applied Biosystems).

Enzyme Preparation and Purification. Human dCK and the various Cys-Ala mutants were cloned into the pET-9d bacterial vector system and transformed into BL21(DE3)pLysS host strains (Novagen, Madison, WI) (*14*). Expression of both coding DNAs was induced by the addition of IPTG, and growth was continued for 4 h at 37 °C. Cells were harvested by centrifugation at 2400*g* (Sorval RC 3C PLUS, Du Pont) for 10 min at 4 °C, resuspended, and lysed by freezing and thawing and sonication for 3 × 1 min on ice in 20 mM Tris-HCl (pH 7.9), 0.5 M NaCl, and 1 mM PMSF. The lysates were centrifuged at 260000*g* (2330 Ultraspin 55, LKB) for 1 h at 4 °C. Wild-type dCK and the various mutant dCKs were then purified by metal chelation affinity chromatography with 0.5 M imidazole in 20 mM Tris-HCl (pH 7.9) and 0.2 M NaCl.

Gel Filtration Chromatography. Gel filtration chromatography was performed using fast protein liquid chromatography on a Superdex 200 column with the Pharmacia Monitor UV-II apparatus (Pharmacia Biotech, Uppsala, Sweden) operating at 280 nm and a flow rate of 1.5 mL/min in a buffer containing 10 mM potassium phosphate buffer (pH 7.3). BSA ($M_r = 66\,000$) and carbonic anhydrase ($M_r = 29\,000$) were used as molecular weight markers. Protein fractions corresponding to an M_r of 60 000 were collected and concentrated with the centrifugal filter device, Ultrafree-15 (Millipore AB).

Enzyme Assay Using Labeled Nucleosides. The activity of dCK was routinely followed by a radiochemical assay procedure as described previously (*1*, *2*) using tritium-labeled substrates [5-^{3}H]dCyd (Amersham Corp., Little Chalfont, U.K.) and [2,8-^{3}H]dAdo (Moravek Biochemical Inc.). The method is based on the measurement of the amount of labeled monophosphate product bound to Whatman DE-81 ion exchange filters (Whatman International Ltd.). Assays were performed in 50 mM Tris-HCl (pH 7.6) or 10 mM potassium phosphate buffer (pH 7.2) containing 100 mM KCl, 5 mM $MgCl_2$, 5 mM ATP, 2 mM DTT, and 0.5 mg/mL BSA. Reactions were initiated by adding the appropriate dCK preparation, and 10 μL portions of the resulting reaction mixtures were removed after 10, 20, and 30 min. K_m and V_{max} values were calculated by fitting velocity data to the Michaelis−Menten equation by nonlinear regression analysis using SigmaPlot Enzyme Kinetic version 7. Each value is the mean of at least three separate determinations.

Labeling of dCK with N-(1-Pyrene)maleimide. Wild-type or mutant dCK was dissolved in 50 mM Tris-HCl buffer (pH 7.5), 100 mM NaCl, 5 mM $MgCl_2$, and 1 mM

Table 2: Kinetic Parameters of Wild-Type dCK and Cys-185-Ala dCK with Variable Phosphate Donors and Constant Phosphate Acceptors[a]

phosphate acceptor	phosphate donor	wild-type K_m[b]	wild-type V_{max}[c]	wild-type K_{ef}[d]	Cys-185-Ala K_m[b]	Cys-185-Ala V_{max}[c]	Cys-185-Ala K_{ef}[d]
dCyd	ATP	19 ± 5	97 ± 8	3.2	25 ± 5	54 ± 3	2.1
	UTP	11 ± 2	42 ± 2	3.9	17 ± 7	43 ± 3	2.5
dAdo	ATP	97 ± 8	669 ± 28	6.9	87 ± 19	652 ± 34	7.5
	UTP	40 ± 4	286 ± 9	7.5	20 ± 5	257 ± 11	13.0

[a] Phosphorylation was followed by the radiochemical method with tritium-labeled nucleosides with variable concentrations of ATP or UTP (5, 20, 80, 250, 500, and 2000 μM) as phosphate donors and a constant concentration of dCyd (10 μM) and dAdo (50 μM) as phosphate acceptors.[b] In micromolar. [c] In nanomoles per minute per milligram. [d] V_{max}/K_m.

dithiothreitol and dialyzed overnight at 4 °C against the same buffer. Subsequently, dialysis was performed overnight at 4 °C against 50 mM Tris-HCl (pH 7.5), 100 mM NaCl, and 5 mM $MgCl_2$, without dithiothreitol. PM (Molecular Probes, Eugene, OR) was dissolved in *N*,*N*-dimethylformamide and the mixture added slowly until an approximate 4-fold molar excess of reagent to protein was achieved. The reaction was allowed to proceed for 2 h at 4 °C in the dark on a mechanical rocker. The reaction mixture was centrifuged at 15000*g* for 10 min to remove the precipitated reagent, and the supernatant was subjected to exhaustive dialysis with several changes against 50 mM Tris-HCl (pH 7.5), 100 mM NaCl, and 5 mM $MgCl_2$ to remove the traces of excess reagent. The extent of labeling of the protein with PM was quantitated by independent determinations of the amounts of PM and protein in the reaction mixture. The pyrene concentration was determined spectrophotometrically using a molar absorption coefficient of 2.3×10^4 M^{-1} cm^{-1} at 344 nm (*15*). The concentration of PM-labeled protein was determined using the Bradford assay (*16*), with bovine serum albumin as a standard.

Fluorescence Studies. Steady-state fluorescence spectra were measured at 25 °C on a Perkin-Elmer LS-55 spectrofluorometer (Freemont) with 5 nm spectral resolution for excitation and emission using 0.5−1.0 μM solutions of purified wild-type or mutant dCK. Protein fluorescence was excited at 295 nm, and fluorescence emission spectra were recorded in the 300−400 nm range; changes in fluorescence were usually monitored at the emission maximum (330 nm). In studying the effects of substrates on protein fluorescence intensities, we made additions to the reaction mixtures from substrate stock solutions, keeping the dilution below 3%, and fluorescence intensities were corrected for dilution factors. Background emission, if present (<3%), was eliminated by subtracting the signal obtained from a buffer solution that contained the appropriate concentration of substrate. The total absorption of protein samples was kept below 0.02 at 295 nm. The quantum yield in the absence and presence of acceptor PM was determined by the comparative method (*17*) with *N*-acetyltryptophanamide as the standard. A value of 0.14 was used as the quantum yield of the standard (*18*).

Fluorescence Resonance Energy Transfer Measurements. Nonradiative energy transfer between Trp residues of wild-type and mutant dCK and PM was followed in these experiments. Addition of PM to the protein mixture, prepared as described above, resulted in quenching of Trp fluorescence, and this was accompanied by the appearance of two sharp monomer pyrene fluorescence peaks at 378 and 396 nm. The estimation of molecular distances by intermolecular energy transfer between the emission transition dipole of a donor molecule and the absorption transition dipole of an appropriate acceptor is based on the theory of Förster (*19*). The rate of energy transfer from a specific donor to a specific acceptor (k_t) is given by

$$k_t = (1/T_d)(R_0/R)^6 \quad (1)$$

where T_d is the lifetime of the donor in the absence of the acceptor, R is the distance between the donor and acceptor, and R_0 is a characteristic distance called the "Förster critical distance" at which the efficiency of transfer is 50%. R_0, which is dependent on spectral properties and the relative orientation of the donor−acceptor pair, can be evaluated from

$$R_0 = (9.79 \times 10^3)(J\kappa^2 Q_D n^{-4})^{1/6}\ \text{Å} \quad (2)$$

where J is the spectral overlap integral of donor fluorescence and acceptor absorbance, Q_D is the quantum efficiency of the donor, n is the refractive index of the medium (taken to be 1.4), and κ^2 is a dipole orientation factor. The value of $^2/_3$ for κ^2 was used on the basis of the assumption of random rotation of the fluorophores (*20*). The overlap integral was approximated by eq 3.

$$J = \sum F_D(\lambda)\epsilon_A(\lambda)\lambda^4\Delta\lambda / \sum F_D(\lambda)\Delta\lambda \quad (3)$$

where $F_D(\lambda)$ is the corrected fluorescence of the donor, $\epsilon_A(\lambda)$ is the molar extinction coefficient of the acceptor, and λ is the wavelength in centimeters. The terms were summed over 2 nm intervals. The efficiency of energy transfer (E) was calculated from changes in fluorescence as follows

$$E = 1 - (Q_{DA}/Q_D) \quad (4)$$

where Q_D and Q_{DA} are the quantum yields of the donor in the absence and presence of acceptor, respectively. The distances between the donor and acceptor were calculated from eq 5.

$$E = (R_0/R)^6/[1 + (R_0/R)^6] \quad (5)$$

RESULTS

Kinetic Studies of Wild-Type and Cys-185-Ala dCK. The capacities of wild-type and Cys-185-Ala dCK to phosphorylate dAdo and dCyd using ATP and UTP as phosphate donors were determined. The resulting kinetic parameters are listed in Table 2. To study the influence of phosphate donors on the nucleoside specificity of dCK, we used an assay that measured activities with variable concentrations of ATP or UTP (5, 20, 80, 250, 500, and 2000 μM) as the phosphate donor and constant concentrations of either dCyd (10 μM) or dAdo (50 μM) as the phosphate acceptor.

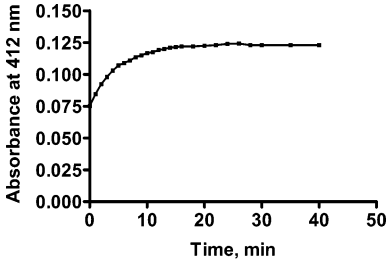

FIGURE 1: Reaction of wild-type dCK and DTNB. The concentration of dCK was 4.3 μM in 50 mM Tris-HCl (pH 7.5), 100 mM NaCl, and 5 mM $MgCl_2$ at 25 °C. Excess DTNB was added (35.0 μM) to the protein, and the change in absorption at 412 nm was monitored as a function of time.

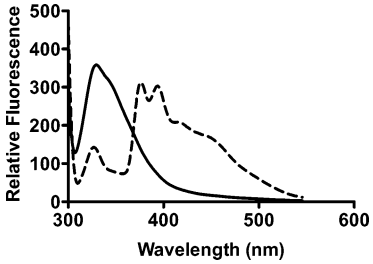

FIGURE 2: Fluorescence emission spectra of wild-type dCK (—) and dCK-PM (− − −). The concentration of dCK was 0.24 μM in 50 mM Tris-HCl (pH 7.5), 100 mM NaCl, and 5 mM $MgCl_2$ at 25 °C. The concentration of PM added was 0.25 μM. The excitation wavelength was 295 nm.

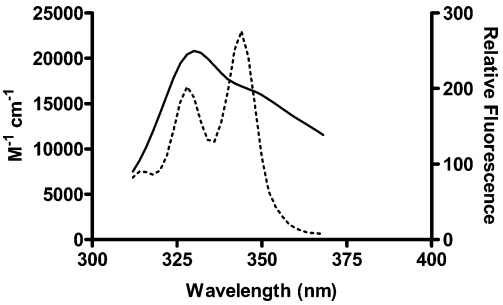

FIGURE 3: Overlap of the Trp emission spectrum of wild-type dCK (—) excited at 295 nm with the absorption of the PM-labeled complex (- - -). The right ordinate gives fluorescence intensities measured in arbitrary units; the left ordinate is calibrated in terms of the molar absorbance of the dCK-PM complex.

Although wild-type and Cys-185-Ala dCK had similar V_{max} and K_m values with the various substrates, there were some important differences. Cys-185-Ala dCK exhibited somewhat lower K_{ef} (V_{max}/K_m) values with dCyd as the substrate with both phosphate donors, whereas it exhibited a K_{ef} value that was nearly 2 times higher than that seen with wild-type dCK with dAdo as the substrate and UTP as the phosphate donor. These results demonstrated that the Cys 185 to Ala substitution reduced the level of dCyd phosphorylation and stimulated dAdo phosphorylation, particularly when UTP was the phosphate donor. The Cys-185-Ala mutant had a somewhat decreased stability during purification and storage (approximately 20% after storage at −70 °C). In previous investigations, we found that substitution of Cys 45 with Ser led to an unstable enzyme that could not be purified and characterized (*14*). Cys-101-Ala dCK and Cys-146-Ala dCK exhibited low activities. Cys-101-Ala dCK exhibited ∼5% of wild-type dCK activity with 25 μM dCyd as well as 50 μM dAdo using 5 mM ATP as the phosphate donor (3.8 nmol of dCMP min^{-1} mg^{-1} and 63 nmol of dAMP min^{-1} mg^{-1}). Cys-146-Ala exhibited ∼1% of wild-type dCK activity with both substrates, i.e., 0.47 nmol of dCMP min^{-1} mg^{-1} and 12 nmol of dAMP min^{-1} mg^{-1}.

Labeling of dCK. PM, which reacts specifically with Cys groups in proteins, was added in 4-fold molar excess to dCK to determine if any of the six Cys residues of dCK could be labeled. The degree of labeling was 1.9 ± 0.2 (mean ± standard error, $n = 4$) mol of PM per mole (monomer weight) of dCK. The sulfhydryl groups in dCK were also titrated with 5,5′-dithiobis(2-nitrobenzoic acid) (DTNB) (Figure 1) as described previously (*21*). The molar equivalent of sulfhydryl groups derivatized per mole of dCK, assuming an extinction coefficient of 13 600 M^{-1} cm^{-1} for the liberated 5-nitro-2-thiobenzoate and a monomer M_r of 30 500, was 2.1 ± 0.1 ($n = 4$). These results indicated that two thiol groups in dCK were accessible for labeling with PM. PM-labeled dCK was functionally active and retained nearly 90% of the activity of unlabeled dCK with either dCyd or dAdo as the phosphate acceptor and ATP as the phosphate donor (data not shown). However, when the protein was denatured in 6 M Gdn-HCl, 5.7 thiol groups were readily available to the reagent, suggesting that under this condition all six sulfhydryl groups reacted with DTNB. The three-dimensional crystal structure of human dCK also revealed no S−S bonds. When the Cys-185-Ala dCK and Cys-146-Ala dCK mutants were subjected to PM labeling under conditions similar to those used for wild-type dCK, the molar equivalents of derivatized sulfhydryl groups per mole of dCK obtained were 1.1 ± 0.1 and 0.8 ± 0.1, respectively, indicating that a single Cys residue was labeled in both instances. These results indicated that Cys 185 and 146 were labeled with PM in wild-type dCK.

The emission spectrum of dCK, when excited at 295 nm at which Tyr and Phe have no absorption and Trp is the only stimulated fluorophore, is shown in Figure 2. The emission maximum was centered at 330 nm. Addition of PM quenched Trp fluorescence at 330 nm, and this was accompanied by the appearance of two sharp fluorescence peaks at 378 and 396 nm. Since free PM does not fluoresce under these experimental conditions, the two peaks observed at 378 and 396 nm represented Trp-excited pyrene fluorescence and demonstrated energy transfer to PM.

Figure 3 shows the emission spectrum of dCK and the absorption spectrum of PM-labeled dCK. There was substantial overlap of the absorbance and emission spectra. The overlap integral J, calculated according to eq 3, was 4.06×10^{-15} cm^3 M^{-1}. Assuming $\kappa^2 = {}^2/_3$, $n = 1.4$, and the quantum yield of the donor emission (dCK) in the absence of the acceptor equals 0.09, the Förster critical distance R_0 was 19.90 Å for dCK-PM. The transfer efficiency was 0.61. The determined values of E and R_0 were used to calculate R, the apparent average distance (18.50 Å) separating the Trp residues from the PM-labeled Cys residues. For the mutant, Cys-185-Ala dCK, the values obtained for J and R_0 were 6.05×10^{-15} cm^3 M^{-1} and 21.30 Å, respectively. The quantum yield of the mutant was 0.105, significantly higher than the value of 0.09 obtained for dCK, suggesting that the tryptophans in the mutant were in a more nonpolar environment, which could account for the lower observed efficiency of energy transfer ($E = 0.53$). The distance separating the single labeled Cys residue from Trp residues was signifi-

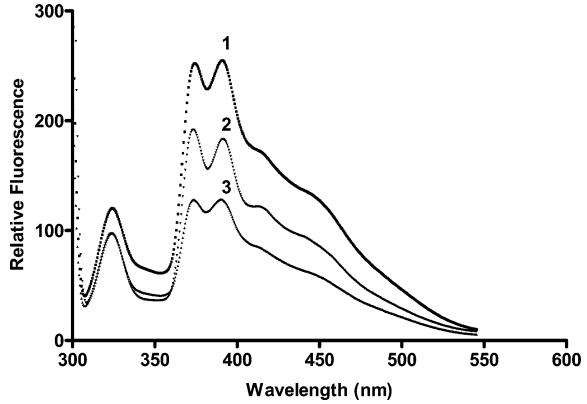

FIGURE 4: Fluorescence emission spectra of wild-type dCK-PM alone (1) or with 10 μM UTP (2) or UTP and dFdC (3). The excitation wavelength was 295 nm, and the concentration of the PM-labeled protein was 0.2 μM.

cantly larger, and the *R* value that was obtained was 20.75 Å.

The emission spectrum of PM-labeled dCK, excited at 295 nm, is shown in Figure 4. The observed fluorescence emission at 330 nm was due to Trp residues, and the two sharp peaks at 378 and 396 nm correspond to Trp-sensitized pyrene monomer fluorescence. Addition of UTP and dFdC quenched the Trp fluorescence of dCK-PM, suggesting an increase in transfer efficiency and providing evidence of a conformational change in dCK-PM upon substrate binding. The effects on transfer efficiencies were measured by determining quantum yields of dCK-PM in the absence and presence of substrates, according to eq 4. The transfer efficiencies were determined to be 0.61 for dCK-PM and 0.70, 0.71, and 0.74 for dCK-PM in the presence of ATP, dFdC, and ATP with dFdC, respectively. The average distances (*R* values) in angstroms between the Trp and Cys residues were determined from the measured *E* values according to eq 5. The average distance *R* for dCK-PM was 18.50 Å, and this distance was reduced to 17.70 and 17.50 Å upon binding of ATP and dFdC, respectively. The *R* value for the ternary complex involving dCK-PM, ATP, and dFdC was 16.80 Å, suggesting that a conformational change in the binary complex occurred when dFdC bound to dCK-PM in the presence of ATP. The energy transfer results obtained with other binary and ternary complexes are listed in Table 3.

Affinities of dCK-PM for Substrates. As shown in Figure 4, binding of substrates to dCK-PM quenched Trp fluorescence (330 nm) and pyrene fluorescence (378 and 396 nm). Because substrate binding resulted in partial fluorescence quenching with no change in the emission maximum, it was possible to determine binding affinities (K_d values) and stoichiometries by following fluorescence quenching as a function of substrate concentration as described previously (*11*). Binding of substrates had a more pronounced effect (quenching) on Trp-sensitized pyrene fluorescence, and for this reason, fluorescence titrations consisted of monitoring changes in fluorescence intensity at 378 nm as a function of substrate concentration. Binding affinities for phosphate donors and purine and pyrimidine nucleoside acceptors are given in Table 4. PM-labeled dCK exhibited a higher affinity for UTP than for ATP with K_d values of 0.36 ± 0.02 and 0.70 ± 0.05 μM, respectively. Among the nucleoside analogues, binding affinities were in the following rank order: dFdC > dCyd > Fara-A (fludarabine) > dAdo. dCK-PM bound nucleoside analogues more tightly in the presence of phosphate donors; e.g., K_d values for dFdC in the absence and presence of UTP were 0.50 ± 0.02 and 0.25 ± 0.01 μM, respectively. These values were slightly lower (higher affinities) than those obtained by monitoring intrinsic Trp fluorescence (*22*). As expected, dCK-PM bound dFdC and dCyd more tightly than dAdo and Fara-A (~4-fold). Fluorescence titrations were also performed by monitoring pyrene fluorescence directly by exciting dCK-PM at 345 nm, a wavelength at which PM is the only excitable fluorophore. The K_d values for ATP and dCyd (0.60 ± 0.04 and 0.45 ± 0.04 μM, respectively) were comparable to those obtained from Trp-sensitized pyrene fluorescence induced by excitation at 295 nm.

We studied the effects of ATP, dFdC, and Fara-A on the conformation of Cys-185-Ala dCK by fluorescence titration. The mutant was excited at 295 nm, and the fluorescence intensity at 330 nm due to Trp was monitored as a function of substrate concentration. Binding of substrates resulted in the partial quenching of Trp fluorescence, and the K_d values for ATP, dFdC, and Fara-A were 1.0 ± 0.05, 1.15 ± 0.05, and 1.50 ± 0.05, μM, respectively, and were comparable to values obtained previously for wild-type dCK (*22*). The extent of Trp fluorescence quenching observed with Cys-

Table 3: Fluorescence Energy Transfer Parameters of PM-Labeled Wild-Type dCK and Cys-185-Ala dCK[a]

	overlap integral J^b (cm^3 M^{-1})	critical distance R_0 (Å)	efficiency of transfer E^c (%)	distance between Trp and Cys R (Å)
dCK	4.06×10^{-15}	19.90	61	18.50
dCK and dFdC	5.08×10^{-15}	20.30	71	17.50
dCK, ATP, and dFdC	5.13×10^{-15}	20.35	74	16.80
dCK, UTP, and dFdC	5.46×10^{-15}	20.75	76	17.10
dCK and dCyd	4.95×10^{-15}	20.21	70	17.75
dCK, ATP, and dCyd	5.50×10^{-15}	20.60	74	17.30
dCK and dAdo	3.97×10^{-15}	19.50	67	17.20
dCK, ATP, and dAdo	5.04×10^{-15}	20.20	70	17.30
dCK and Fara-A	4.00×10^{-15}	19.50	69	17.25
dCK, ATP, and Fara-A	4.70×10^{-15}	20.05	73	17.35
ATP	5.06×10^{-15}	20.50	70	17.70
UTP	5.26×10^{-15}	20.80	72	17.90
Cys-185-Ala dCK	6.05×10^{-15}	21.30	53	20.75

[a] All measurements were carried out at 25 °C in 50 mM Tris (pH 7.5), 100 mM NaCl, and 5 mM $MgCl_2$. [b] Determined as described in Materials and Methods. [c] Energy transfer efficiency calculated from changes in fluorescence intensity. The relative errors in the *R* values are ±0.1 Å.

Table 4: Binding of Substrates to Wild-Type dCK-PM[a]

ligand	K_d (μM)	ligand	K_d (μM)
ATP	0.70 ± 0.05	UTP and dFdC	0.25 ± 0.01
UTP	0.36 ± 0.02	dAdo	2.10 ± 0.10
dCyd	0.75 ± 0.05	ATP and dAdo	1.50 ± 0.10
ATP and dCyd	0.50 ± 0.05	Fara-A	1.80 ± 0.10
dFdC	0.50 ± 0.02	ATP and Fara-A	1.40 ± 0.10
ATP and dFdC	0.40 ± 0.02		

[a] Experiments were conducted using 0.4 μM labeled protein at 25 °C in 50 mM Tris (pH 7.5), 100 mM NaCl, and 5 mM $MgCl_2$. K_d values (means ± standard error, $n = 3$) were determined by fluorescence titration of pyrene fluorescence at 378 nm, with excitation of at 295 nm.

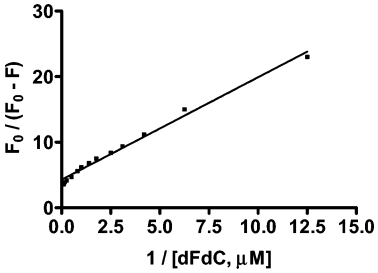

FIGURE 5: Modified Stern−Volmer plot of the steady-state quenching of Trp fluorescence of Cys-185-Ala dCK by dFdC. The decrease in fluorescence ($F_0 - F$) at an emission wavelength of 330 nm is expressed as a fraction of the unquenched fluorescence F_0 and is plotted as a function of the reciprocal ligand concentration. The excitation wavelength was 295 nm.

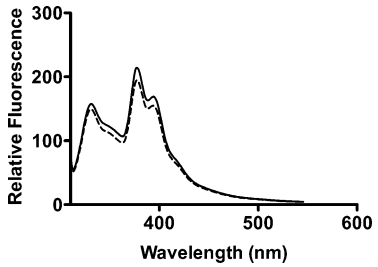

FIGURE 6: Fluorescence emission spectra of Cys-185-Ala-PM dCK in the absence (—) and presence of 10 μM dFdC (− − −). The PM-labeled mutant was excited at 295 nm, and the protein concentration was 0.2 μM in 50 mM Tris-HCl (pH 7.5), 100 mM NaCl, and 5 mM $MgCl_2$ at 25 °C.

185-Ala dCK was considerably lower (25−30%) than that observed with wild-type dCK (60−70%), suggesting that the Trp residues in the mutant protein were less accessible to the substrates. The fractional accessibilities of Trp residues (f_a) in wild-type and mutant dCK were determined (Figure 5) using the modified Stern−Volmer equation (*23*). The values of f_a determined for wild-type dCK with ATP, Fara-A, and dFdC were 0.48, 0.45, and 0.55, respectively, whereas the corresponding values determined for Cys-185-Ala dCK were 0.25, 0.23, and 0.30, respectively. This finding was consistent with the differences observed in the quantum values for wild-type and mutant dCK (0.09 and 0.105, respectively), suggesting that the Trp residues in Cys-185-Ala were in a more nonpolar environment (i.e., shielded from the solvent) than in wild-type dCK.

When Cys-185-Ala-PM dCK was excited at 295 nm, it exhibited an emission spectrum similar to that of dCK-PM (Figure 6). The spectrum was characterized by Trp fluorescence at 330 nm and pyrene fluorescence peaks at 378 and 396 nm. Binding of ATP, dAdo, dCyd, or dFdC to Cys-185-Ala-PM dCK had little, if any, effect on pyrene fluorescence with quenching of ~5%, whereas binding of these ligands to dCK-PM produced ~40% quenching. Thus, the observed conformational changes reflected by pyrene fluorescence upon binding of substrates to dCK-PM can be attributed to Cys 185 since its removal by mutation to Ala greatly reduced the substrate-induced conformational changes without significantly affecting its functional activity. The Cys-146-Ala-PM dCK mutant, when excited at 295 nm, also had an emission spectrum similar to that of dCK-PM. Addition of substrates (dAdo, dCyd, or dFdC) had no significant effect on pyrene fluorescence (quenching of <3%), in agreement with our functional assays, since this mutant was found to have a very low activity compared to that of wild-type dCK, suggesting that replacement of Cys with Ala at this position directly interfered with binding of the substrate to dCK.

DISCUSSION

Deoxyribonucleoside kinases phosphorylate deoxyribonucleosides and activate a number of medically important nucleoside analogues, and their impairment inevitably results in drug resistance (*24*). The initial 5′-phosphorylation carried out by nucleoside kinases is the rate-limiting step in the activation of nucleoside drugs. The single most important nucleoside kinase for activation of anticancer drugs is dCK. The critical function of dCK in cancer chemotherapy is evident from a direct correlation between dCK activity and drug sensitivity in tumor cell lines (*25*). Although dCyd is the preferred physiological substrate for dCK, it also phosphorylates dGuo and dAdo. In addition, dCK activates a number of clinically established prodrugs, including AraC, F-araC, cladribine, dFdC, and troxcitabine. It has been suggested that dCK can exist in different conformational states depending upon the substrates, and this may account for its broad substrate specificity (*5*, *11*, *22*).

Sabini et al. (*5*) have determined the three-dimensional crystal structure of human dCK to a resolution of 1.6 Å in complex with its physiological substrate dCyd and with the prodrugs AraC and dFdC. In this study, we detected the effects of binding of phosphate donors and nucleoside analogues on the conformation of dCK by steady-state fluorescence energy transfer measurements, which allowed determination of distances between specific sites on the enzyme (*26*, *27*). Since there was a good overlap between the emission spectrum of the donor with the absorption spectrum of the acceptor, the Trp residues in dCK were used as the energy donors and the PM attached to Cys residues was used as the energy acceptor. The fluorescent probe PM binds in the proximity of Trp residues, which is reflected by quenching by PM on the fluorescence emission of Trp without any alteration of its emission maximum and the demonstration that PM is also the recipient of intrinsic energy from Trp. Earlier studies have shown that dCK undergoes a conformational change involving Trp residues upon binding of its substrates (*10*, *11*).

There are seven tryptophan residues in dCK, which are more or less evenly positioned throughout the protein. An R value so close to the R_0 value suggests that a significant amount of fluorescence from donors must be lost as nonradiative energy with the result being that the average distance R is close to the R_0 value. Of the seven tryptophans in dCK, only Trp 58 and 215 are 15.85 and 15.60 Å, respectively, from Cys 185, values which corresponded to the calculated R_0 value of 16.25 Å. The other five tryptophans are at greater distances ranging from 21.75 to 34.20 Å and are unlikely to make a significant contribution to the observed conformational changes.

The structures of the deoxynucleoside kinases (dNKs), deoxyguanosine kinase (dGK), and dCK monomers are similar (*5*, *24*). In the dNK structure, which was determined with crystals containing the substrate dCyd, the base makes π-interactions by stacking with Phe 114, while the other side of the base interacts with Trp 57 and Phe 80. The corre-

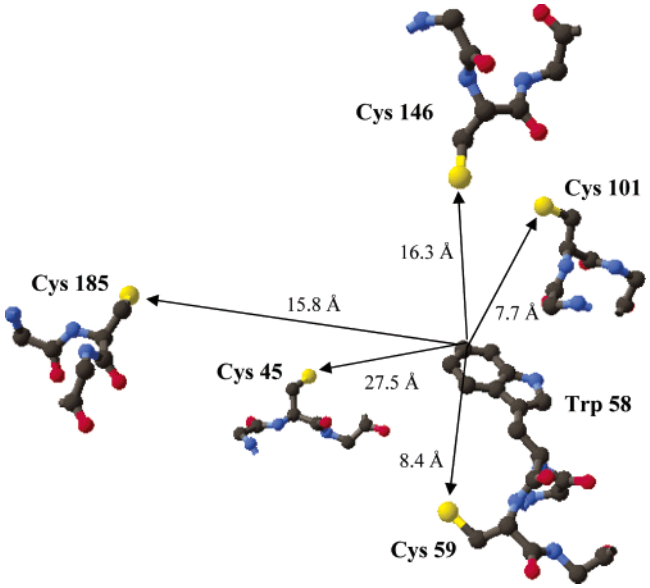

FIGURE 7: Locations of Cys residues and Trp 58 in the human dCK three-dimensional structure (PDB entry 1p60). The arrows show the distances between Trp 58 and Cys 45, 59, 101, 146, and 185, using SwissPdbViewer version 3.7b. The measurement was from C5 of the indole ring of Trp 58.

sponding residue in dCK is Trp 58, which is 4.1 Å from Arg 104 at the active site (*24*), whereas Trp 215 is 14.90 Å from Arg 104. Hence, the observed conformational changes upon substrate binding, resulting in the loss in energy transfer, are likely attributed to Trp 58. Binding of substrates (dCyd, dFdC, ATP, and UTP) perturbed a single Trp residue in dCK, which became more exposed to solvent as a consequence of substrate binding as revealed by UV difference spectroscopy (*11*). In this study, the observed quenching in Trp fluorescence emission and the reduction in quantum yield upon binding substrates to dCK-PM also suggest that the Trp residue becomes more exposed in the presence of substrates. Hence, the observed conformational changes involving Trp quenching in dCK-PM upon substrate binding were most likely due to the perturbation of Trp 58.

There are six Cys residues in the amino acid sequence of human dCK, and Cys 185 and 146 are potential candidates for PM labeling on the basis of their proximity to Trp 58 in the three-dimensional crystal structure (Figure 7). Cys 185 is in α-helix 7, near the LID region, which is directly involved in substrate binding. One side of α-helix 7, between Gln 179 and Gln 199, binds the phosphate donors by forming the top of the active site and interacts with the triphosphate groups of ATP and/or UTP. This region has previously been shown to affect selectivity for nucleoside substrates and phosphate donors as demonstrated by the properties of triple mutant R179/K184/N187 (*14*). Changing Cys 185 to Ala may have affected interactions between amino acids in α-helix 7 and residues in the LID region. The kinetic properties of Cys-185-Ala dCK differed from those of wild-type dCK in that dAdo phosphorylation with UTP as the phosphate donor was enhanced whereas dCyd phosphorylation was inhibited. This kinetic profile is similar to that of triple mutant R179/K184/N187, which is also altered in the LID region to mimic the situation in mouse dCK (*14*).

The identity of the second Cys labeled with PM is most likely Cys 146, since this is the only Cys in the vicinity of Trp 58 and Cys 185 (Figure 7) that matches the distances measured here by the fluorescence transfer method. Another candidate, Cys 9, is not seen in the three-dimensional structure and thus is unlikely to be in the proximity of the active site Trp. Cys 45 is farther from Trp 58 than the other Cys residues, whereas Cys 59 and Cys 101 are much closer than the measured distances. As mentioned above, Cys-101-Ala dCK had only 5% activity compared to wild-type dCK, suggesting that the substitution of Ala at this position interfered directly with substrate binding. In addition, when the Cys-185-Ala dCK and Cys-146-Ala dCK mutants were subjected to PM labeling, only a single sulfhydryl group per mole of dCK was labeled with both mutants, strongly suggesting that Cys 185 and 146 were labeled with PM in wild-type dCK. The fact that the Cys-146-Ala dCK mutant had very low activity suggests that replacement of Cys with an Ala residue at this position interfered directly with substrate binding; as a consequence, addition of substrates had no significant effect on Cys-146-Ala-PM dCK protein fluorescence. Even though Cys 185 is labeled in this mutant (Cys-146-Ala-PM dCK), we observed no change in pyrene fluorescence upon substrate addition, thus demonstrating that the observed conformational changes upon substrate binding in wild-type dCK primarily arise from the perturbation of the pyrene label at Cys 185.

The environment of Trp 58 in Cys-185-Ala dCK is more nonpolar than in wild-type dCK, and as a consequence, binding of ligands produced considerably less quenching of Trp fluorescence. Accordingly, the replacement of Cys 185 with Ala affected the environment of Trp 58 in the active-site region. The measured distance between the Trp residues and the two PM-labeled Cys residues in dCK-PM was 18.50 Å, whereas the measured distance between the donor and the single PM-labeled Cys residue in Cys-185-Ala-PM dCK was 20.75 Å. Hence, the calculated distance between the donor (Trp 58) and the acceptor (PM-labeled Cys 185) in dCK-PM was 16.25 Å, in good agreement with the three-dimensional crystallographic data (Figure 7). The values of *R*, the measured distances between the donor and acceptor for dCK-PM and Cys-185-Ala-PM dCK, suggest high efficiencies of energy transfer. The *E* values for dCK-PM and Cys-185-Ala-PM dCK were consistent with their *R* values. In Cys-185-Ala-PM dCK, the PM-labeled single Cys residue was farther away (20.75 Å) than in doubly labeled dCK-PM (18.50 Å), and the mutant therefore had a lower *E* value (0.53) than dCK-PM (0.61). When different substrates bound, dCK-PM assumed different conformational states as revealed by the *R* values. There was also clear evidence of the formation of binary and ternary complexes. For example, the *R* values obtained with dFdC in the absence (binary complex) and presence (ternary complex) of ATP were 17.5 and 16.80 Å, respectively. Also, the nature of the ternary complexes formed with dCyd and dFdC was different from the nature of those obtained with dAdo and Fara-A. In the case of dCyd and dFdC, the *R* values for the ternary complexes were significantly lower than the corresponding values for the binary complexes. It is conceivable that the observed differences in the conformational states of the binary and ternary complexes of wild-type dCK with purine and pyrimidine nucleoside analogues may account for its substrate specificity. Our results agree with the recent model of the purine nucleoside binding form of dCK (*12*) in which

the active site was larger that that reported for the structurally determined pyrimidine nucleoside binding form (*12*).

In summary, we have demonstrated by fluorescence energy transfer measurements that recombinant human dCK undergoes a conformational change upon substrate binding. Binding of substrates perturbed the environments of Trp and Cys residues. In dCK-PM, the measured average distance between Trp 58 and Cys 185 and 146 varied with the substrates. In the PM-labeled mutant protein, Cys-185-Ala-PM dCK, binding of substrates had no significant effect on pyrene fluorescence, suggesting that the observed conformational changes involving labeled Cys residues in dCK-PM occurred because of the perturbation of Cys 185 near the lid region and that Cys 146 is in a much less mobile part of the active site of dCK.

REFERENCES

1. Eriksson, S., and Wang, L. (1997) Substrate specificity, expression, and primary sequences of deoxynucleoside kinases, implications for chemotherapy, *Nucleosides Nucleotides 16*, 653−659.
2. Usova, E. V., and Eriksson, S. (1997) The effects of high salt concentrations on the regulation of the substrate specificity of human recombinant deoxycytidine kinase, *Eur. J. Biochem. 248*, 762−766.
3. Eriksson, S., Kierdaszuk, B., Munch-Petersen, B., Oberg, B., and Johansson, N. G. (1991) Comparison of the substrate specificities of human thymidine kinase 1 and 2 and deoxycytidine kinase toward antiviral and cytostatic nucleoside analogs, *Biochem. Biophys. Res. Commun. 176*, 586−592.
4. Chottiner, E. G., Shewach, D. S., Datta, N. S., Ashcraft, E., Gribbin, D., Ginsburg, D., Fox, I. H., and Mitchell, B. S. (1991) Cloning and expression of human deoxycytidine kinase cDNA, *Proc. Natl. Acad. Sci. U.S.A. 88*, 1531−1535.
5. Sabini, E., Ort, S., Monnerjahn, C., Konrad, M., and Lavie, A. (2003) Structure of human dCK suggests strategies to improve anticancer and antiviral therapy, *Nat. Struct. Biol. 10*, 513−519.
6. Bohman, C., and Eriksson, S. (1988) Deoxycytidine kinase from human leukemic spleen: Preparation and characteristics of homogeneous enzyme, *Biochemistry 27*, 4258−4265.
7. Ives, D. H., and Durham, J. P. (1970) Deoxycytidine kinase. 3. Kinetics and allosteric regulation of the calf thymus enzyme, *J. Biol. Chem. 245*, 2285−2294.
8. Hughes, T. L., Hahn, T. M., Reynolds, K. K., and Shewach, D. S. (1997) Kinetic analysis of human deoxycytidine kinase with the true phosphate donor uridine triphosphate, *Biochemistry 36*, 7540−7547.
9. Shewach, D. S., Reynolds, K. K., and Hertel, L. (1992) Nucleotide specificity of human deoxycytidine kinase, *Mol. Pharmacol. 42*, 518−524.
10. Kierdaszuk, B., Rigler, R., and Eriksson, S. (1993) Binding of substrates to human deoxycytidine kinase studied with ligand-dependent quenching of enzyme intrinsic fluorescence, *Biochemistry 32*, 699−707.
11. Mani, R. S., Usova, E. V., Eriksson, S., and Cass, C. E. (2003) Hydrodynamic and Spectroscopic Studies of Substrate Binding to Human Recombinant Deoxycytidine Kinase, *Nucleosides, Nucleotides Nucleic Acids 22*, 175−192.
12. Johnsamuel, J., Eriksson, S., Oliveira, M., and Tjarks, W. (2005) Docking simulation with a purine nucleoside specific homology model of deoxycytidine kinase, a target enzyme for anticancer and antiviral therapy, *Bioorg. Med. Chem. 13*, 4160−4167.
13. Ho, S. N., Hunt, H. D., Horton, R. M., Pullen, J. K., and Pease, L. R. (1989) Site-directed mutagenesis by overlap extension using the polymerase chain reaction, *Gene 77*, 51−59.
14. Usova, E. V., and Eriksson, S. (2002) Identification of residues involved in the substrate specificity of human and murine dCK, *Biochem. Pharmacol. 64*, 1559−1567.
15. Betcher-Lange, S. L., and Lehrer, S. S. (1978) Pyrene excimer fluorescence in rabbit skeletal α,α-tropomyosin labeled with N-(1-pyrene)maleimide. A probe of sulfhydryl proximity and local chain separation, *J. Biol. Chem. 253*, 3757−3760.
16. Bradford, M. M. (1976) A rapid and sensitive method for the quantitation of microgram quantities of protein utilizing the principle of protein-dye binding, *Anal. Biochem. 72*, 248−254.
17. Parker, C. A., and Reese, W. T. (1960) Correction of fluorescence spectra and measurement of fluorescence quantum efficiency, *Analyst (London) 85*, 587−592.
18. Eftink, M. R., Jia, Y., and Hu, D. (1995) Fluorescence Studies with Tryptophan Analogues: Excited-State Interaction Involving the Side Chain Amino Group, *J. Phys. Chem. 99*, 5713−5723.
19. Förster, T. (1965) in *Modern Quantum Chemistry, Istanbul Lectures*, Academic Press, New York.
20. Selvin, P. R. (1995) Fluorescence resonance energy transfer, *Methods Enzymol. 246*, 300−334.
21. Mani, R. S., and Kay, C. M. (1985) A fluorimetry study of N-(1-pyrenyl)iodoacetamide-labeled bovine brain S-100a protein, *FEBS Lett. 181*, 275−280.
22. Mani, R. S., Usova, E. V., Eriksson, S., and Cass, C. E. (2004) Fluorescence studies of substrate binding to human recombinant deoxycytidine kinase, *Nucleosides, Nucleotides Nucleic Acids 23*, 1343−1346.
23. Lehrer, S. S., and Leavis, P. C. (1978) Solute quenching of protein fluorescence, *Methods Enzymol. 49*, 222−236.
24. Johansson, K., Ramaswamy, S., Ljungcrantz, C., Knecht, W., Piskur, J., Munch-Petersen, B., Eriksson, S., and Eklund, H. (2001) Structural basis for substrate specificity of cellular deoxyribonucleoside kinases, *Nat. Struct. Biol. 8*, 616−620.
25. Hapke, D. M., Stegmann, A. P., and Mitchell, B. S. (1996) Retroviral transfer of deoxycytidine kinase into tumor cell lines enhances nucleoside toxicity, *Cancer Res. 56*, 2343−2347.
26. Wu, C. W., and Stryer, L. (1972) Proximity relationships in rhodopsin, *Proc. Natl. Acad. Sci. U.S.A. 69*, 1104−1108.
27. Cheung, H. C., Gonsoulin, F., and Garland, F. (1983) Fluorescence energy transfer studies on the proximity of the two essential thiols of myosin subfragment-1, *J. Biol. Chem. 258*, 5775−5786.

BI052652B